Relationship between incident angle and dispersion in static large field of view polarization interference imaging spectrometer*

Wu Jun-Fang(吴俊芳)[a)b)] and Zhang Chun-Min(张淳民)[a)†]

[a)] *School of Science, Xi'an Jiaotong University, Xi'an* 710049, *China*
[b)] *School of Science, Xi'an Polytechnic University, Xi'an* 710048, *China*

(Received 6 February 2009; revised manuscript received 40 April 2009)

The static large field of the view polarization interference imaging spectrometer is based on the modified Savart polariscope. There appears a dispersion between the ordinary ray and extraordinary ray when light passes through the modified Savart polariscope. The dispersion greatly influences the intensities and the results of the interferogram and target image in the static large field of the view polarization interference imaging spectrometer. At the same time, the incident angle determines the dispersion. When the light goes through the modified Savart polariscope, the dispersion occurs in the left plate, the half-wave plate and the right plate of the modified Savart polariscope. Using the extension of Snell's law, the dispersion in the crystal is theoretically calculated and numerically simulated separately. The relationship curve between incident angle and the dispersion is obtained by simulation.

Keywords: imaging spectroscopy, dispersion, the modified Savart polariscope
PACC: 4210Q, 4110H, 0765

1. Introduction

In the 1990s, polarization interference imaging spectroscopy emerged. In 2000 the static large field of the view polarization interference imaging spectrometer (SLPIIS) was presented by Zhang *et al.*[1−6] The primary feature of SLPIIS is the large angle of incidence. The target image can be obtained in a spatial domain and the interferogram can be recorded by a two-dimensional CCD camera at the same time. The SLPIIS is widely used in the fields of space and temporal information survey, communication, and metrologies.

The key component in the SLPIIS is a modified Savart polariscope which is made up of crystal. When the light goes through the modified Savart polariscope, it obeys the extension of Snell's law. At the same time, there appears a dispersion between the ordinary ray (*o*-ray) and extraordinary ray (*e*-ray). The dispersion greatly influences the intensities and the results of the interferogram and target image. The study on dispersion of modified Savart polariscope has not been reported by now.

In the present paper, the dispersions occurring in the left plate, the half-wave plate and the right plate of the modified Savart polariscope are theoretically calculated and numerically simulated separately. Using the extension of Snell's law, the dispersion in the crystal is also theoretically calculated and numerically simulated separately. The relationship curve between incident angle and dispersion is obtained by simulation.

2. Static large field of view polarization interference imaging spectrometer

Figure 1 shows an optical layout of the developed SLPIIS. An object located at an infinite distance is imaged on the back focal plane of lens L_0 and the front focal plane of lens L_1. This image is the image of detected target of the system. The CCD camera is located on the back focal plane of lens L_2. The polarizer P_1, the modified Savart polariscope, and the

*Project supported by the State Key Program of National Natural Science of China (Grant No. 40537031), National High Technology Research and Development Program of China (Grant No. 2006AA12Z152), the National Natural Science Foundation of China (Grant Nos. 40875013, 40375010 and 60278019), the Science and Technology Plan Foundation of Shaanxi Province, China (Grant No. 2005K04-G18).
†Corresponding author. E-mail: zcm@mail.xjtu.edu.cn
© 2010 Chinese Physical Society and IOP Publishing Ltd

analyzer P_2 are placed between lens L_1 and lens L_2 The fore-optical system (lenses L_0 and L_1) collimates the input rays and then the rays are polarized by a linear polarizer P_1 and consequently split into two polarized components by a modified Savart polariscope. The modified Savart polariscope shears the two components laterally. The analyzer P_2 is used to ensure that the two components have the same vibrating directions, and lens L_2 converges these two components into its focal plane. The interferogram and the target image in the spatial domain are recorded by an area array detector.

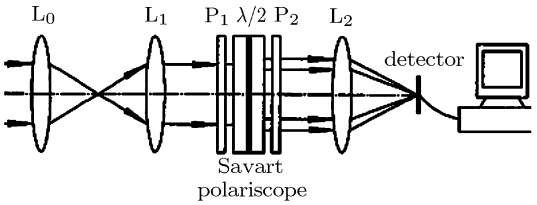


Fig. 1. Optical layout of SLPIIS based on a modified Savart polariscope.

The key component in the SLPIIS is a modified Savart polariscope, which is shown in Fig. 2. It is made up of two identical plates cut at 45° with respect to the optical axes and with their principle sections being parallel; the two optical axes are perpendicular to each other. A half-wave plate is inserted between the left plate and the right plate of the polariscope.

In the first plate the incident ray is divided into two rays *o*-ray and *e*-ray. Because the half-wave plate causes a 90° rotation of the linear polarization states for each of the incident rays, *o*-ray in the first plate becomes *e*-ray in the second plate, and vice versa.[7]

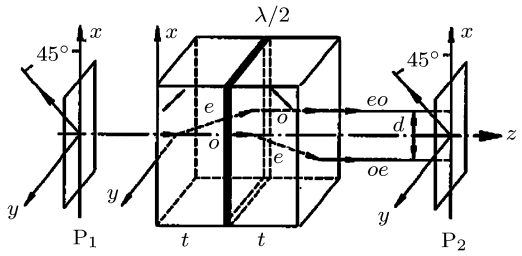


Fig. 2. Modified Savart polariscope.

3. Relationship between incident angle and dispersion in SLPIIS

A light strikes on the modified Savart polariscope at incident angle θ_1. The incident plane is $x-z$ plane, where the z axis is in the crystal surface normal direction. The angle between optical axis and z-axis is θ_p; φ_p is the angle between the projection of optical axis in the $x-y$ plane (crystal surface) and x-axis (that is the angle between the principal section crossed and the incident plane). Let the $\boldsymbol{i}$, $\boldsymbol{j}$ and $\boldsymbol{k}$ are the unit vectors of x, y and z directions respectively, the optical axis direction can be expressed as[8,9]

$$\boldsymbol{e}_p = \sin\theta_p\cos\varphi_p\boldsymbol{i} + \sin\theta_p\sin\varphi_p\boldsymbol{j} + \cos\theta_p\boldsymbol{k}. \quad (1)$$

3.1. Relationship between incident angle and dispersion in the left plate of modified Savart polariscope

The optical axis direction of left plate in modified Savart polariscope is

$$\boldsymbol{e}_p = \frac{\sqrt{2}}{2}\boldsymbol{i} + \frac{\sqrt{2}}{2}\boldsymbol{k}. \quad (2)$$

From expressions (1) and (2), a formula is obtained as follows:

$$\sin\theta_p\cos\varphi_p\boldsymbol{i} + \sin\theta_p\sin\varphi_p\boldsymbol{j} + \cos\theta_p\boldsymbol{k} = \frac{\sqrt{2}}{2}\boldsymbol{i} + \frac{\sqrt{2}}{2}\boldsymbol{k}. \quad (3)$$

So, the values of θ_p and φ_p are obtained as follows:

$$\begin{cases} \theta_p = \dfrac{\pi}{4}, \\ \varphi_p = 0. \end{cases} \quad (4)$$

The *o*-ray obeys the Snell law, and it propagates as in an isotropic material. The angle of refraction is

$$\theta_o = \arcsin(n_1\sin\theta_1/n_o), \quad (5)$$

where n_o is the refractive index of the crystal, n_1 is the refractive index of the air.

3.1.1. Calculation relationship between incident angle and dispersion

3.1.1.1. Direction of *e*-wave vector

The θ_k is the angle between *e*-wave vector and normal of crystal surface, the *e*-wave vector is in the incident plane. The direction of *e*-wave vector is

$$\boldsymbol{e}_k = \sin\theta_k\boldsymbol{i} + \cos\theta_k\boldsymbol{k}. \quad (6)$$

For the *e*-ray, the refractive index in the modified Savart polariscope is expressed as

$$n_2 = \frac{n_o n_e}{\sqrt{n_o^2\sin^2\theta_{kp} + n_e^2\cos^2\theta_{kp}}}, \quad (7)$$

where n_e is the refractive index of the crystal, and θ_{kp} is the angle between the wave vector and the optical axis, θ_{kp} is expressed as[8−15]

$$\cos\theta_{kp} = \boldsymbol{e}_k \cdot \boldsymbol{e}_p = \frac{\sqrt{2}}{2}\left(\sin\theta_k + \cos\theta_k\right). \tag{8}$$

The extension of Snell's law is

$$n_1 \sin\theta_1 = \frac{n_o n_e}{\sqrt{n_o^2 \sin^2\theta_{kp} + n_e^2 \cos^2\theta_{kp}}} \sin\theta_k, \tag{9}$$

where θ_k is the angle between the e-wave vector and the normal of the crystal surface. Using the relation $1/\cos^2\theta_k = 1 + \tan^2\theta_k$, expression (9) is rewritten as

$$\begin{aligned}&\left[\frac{1}{2}\left(n_1\sin\theta_1\right)^2\left(n_e^2+n_o^2\right) - n_o^2 n_e^2\right]\tan^2\theta_k \\ &+ \left(n_1\sin\theta_1\right)^2\left(n_e^2 - n_o^2\right)\tan\theta_k \\ &+ \frac{1}{2}\left(n_1\sin\theta_1\right)^2\left(n_e^2+n_o^2\right) = 0.\end{aligned} \tag{10}$$

Let

$$A_1 = n_1 \sin\theta_1, \tag{11}$$

$$A = n_o^2 n_e^2 - \frac{1}{2}A_1^2\left(n_e^2 + n_o^2\right), \tag{12}$$

$$B = A_1^2\left(n_e^2 - n_o^2\right), \tag{13}$$

$$C = \frac{1}{2}A_1^2\left(n_e^2 + n_o^2\right). \tag{14}$$

Then expression (9) is rewritten as

$$-A\tan^2\theta_k + B\tan\theta_k + C = 0. \tag{15}$$

The solution of Eq. (15) is

$$\tan\theta_k = \frac{1}{2A}\left(B + \sqrt{B^2 + 4AC}\right). \tag{16}$$

3.1.1.2. Direction of e-ray

The angle between the e-ray and the optical axis, and θ_{rp} satisfies the following relationship:

$$\tan\theta_{rp} = \left(n_o^2/n_e^2\right)\tan\theta_{kp}. \tag{17}$$

The direction of e-ray is

$$\boldsymbol{e}_r = \alpha\boldsymbol{e}_k + \beta\boldsymbol{e}_p, \tag{18}$$

where

$$\boldsymbol{e}_r \cdot \boldsymbol{e}_p = \cos\theta_{rp}, \tag{19}$$

and

$$\boldsymbol{e}_r \cdot \boldsymbol{e}_r = 1. \tag{20}$$

Using expressions (8), (18)–(20), the following equation is obtained:

$$\begin{cases}\alpha^2 + 2\alpha\beta\cos\theta_{kp} + \beta^2 = 1, \\ \alpha\cos\theta_{kp} + \beta = \cos\theta_{rp}.\end{cases} \tag{21}$$

The solution of Eq. (21) is

$$\begin{cases}\alpha = \dfrac{n_o^2}{n_e^2}\dfrac{1}{\sqrt{\cos^2\theta_{kp} + \left(n_o^4/n_e^4\right)\sin^2\theta_{kp}}}, \\ \beta = \left(1 - \dfrac{n_o^2}{n_e^2}\right)\dfrac{\cos\theta_{kp}}{\sqrt{\cos^2\theta_{kp} + \left(n_o^4/n_e^4\right)\sin^2\theta_{kp}}}.\end{cases} \tag{22}$$

The direction of e-ray is

$$\boldsymbol{e}_r = \left(\alpha\sin\theta_k + \frac{\sqrt{2}}{2}\beta\right)\boldsymbol{i} + \left(\alpha\cos\theta_k + \frac{\sqrt{2}}{2}\beta\right)\boldsymbol{k}. \tag{23}$$

3.1.1.3. The dispersion of e-ray and o-ray

The thickness of the left plate is t, the coordinate of output o-ray is

$$\begin{cases}x_o = t\tan\theta_o, \\ y_o = 0, \\ z_o = t.\end{cases} \tag{24}$$

Let r be the distance between incident point and exit point, then the coordinate of output e-ray will be

$$\begin{cases}x_e = r\left(\alpha\sin\theta_k + \dfrac{\sqrt{2}}{2}\beta\right), \\ y_e = 0, \\ z_e = r\left(\alpha\cos\theta_k + \dfrac{\sqrt{2}}{2}\beta\right).\end{cases} \tag{25}$$

From $z_e = t$, the r is equal to

$$r = \frac{t}{\alpha\cos\theta_k + \dfrac{\sqrt{2}}{2}\beta}. \tag{26}$$

The dispersion is

$$x = x_e - x_o = \frac{t\left(\alpha\sin\theta_k + \dfrac{\sqrt{2}}{2}\beta\right)}{\alpha\cos\theta_k + \dfrac{\sqrt{2}}{2}\beta} - t\tan\theta_o. \tag{27}$$

3.1.2. Simulation relationship between incident angle and dispersion

For $n_1 = 1.00000$, $n_o = 1.65835$, $n_e = 1.48640$, and $t = 6$ mm, the dispersion curve is shown in Fig. 3. From the figure, the dispersion becomes bigger with the incident angle increasing from 0 to 1.6 rad. In SLPIIS, the dispersion determines the image quality.

Increasing incident angle is one of methods to improve the SLPIIS.

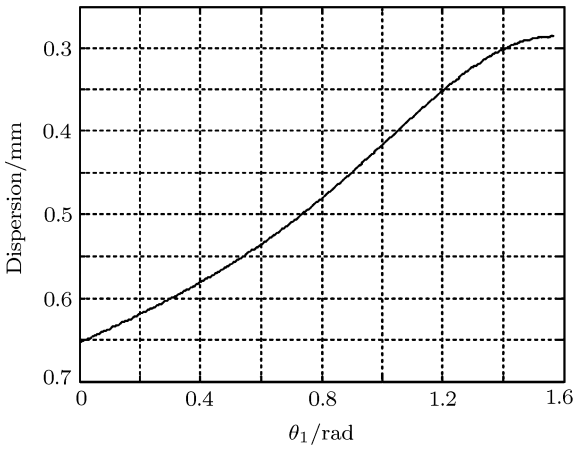


Fig. 3. Relation curve between incident angle and dispersion in the left plate.

3.2. Relationship between incident angle and dispersion in the half-wave plate of modified Savart polariscope

The optical axis direction of the half-wave plate in the modified Savart polariscope is

$$\boldsymbol{e}_p = \frac{\sqrt{2}}{2}\boldsymbol{i} + \frac{\sqrt{2}}{2}\boldsymbol{j}. \tag{28}$$

From expressions (1) and (28), the values of θ_p and φ_p are

$$\begin{cases} \theta_p = \dfrac{\pi}{2}, \\ \phi_p = \dfrac{\pi}{4}. \end{cases} \tag{29}$$

The o-ray obeys the Snell law, and it propagates as in an isotropic material. The angle of refraction is

$$\theta_o = \arcsin(n_1 \sin\theta_1 / n_o), \tag{30}$$

where n_1 is the refractive index of the adherent.

3.2.1. Calculation relationship between incident angle and dispersion

In the same way as that in the left plate in the modified Savart polariscope, we can obtain the direction of e-wave vector

$$\boldsymbol{e}_k = \sin\theta_k \boldsymbol{i} + \cos\theta_k \boldsymbol{k}, \tag{31}$$

where θ_k satisfies the following relationship:

$$\theta_k = \arctan\left(\frac{1}{2n_o^2 n_e^2 - n_1^2\,(n_e^2 + n_o^2)\sin^2\theta_1}\right). \tag{32}$$

The direction of e-ray is

$$\boldsymbol{e}_r = \left(\alpha\sin\theta_k + \frac{\sqrt{2}}{2}\beta\right)\boldsymbol{i} + \frac{\sqrt{2}}{2}\beta\boldsymbol{j} + \alpha\cos\theta_k\boldsymbol{k}. \tag{33}$$

The thickness of the half-wave plate is t', and the coordinate of output o-ray is

$$\begin{cases} x_o = t'\tan\theta_o, \\ y_o = 0, \\ z_o = t'. \end{cases} \tag{34}$$

The coordinate of output e-ray is

$$\begin{cases} x_e = r\left(\alpha\sin\theta_k + \dfrac{\sqrt{2}}{2}\beta\right), \\ y_e = \dfrac{\sqrt{2}}{2}r\beta, \\ z_e = r\alpha\cos\theta_k. \end{cases} \tag{35}$$

The dispersion is

$$\begin{cases} x = \dfrac{t'\left(\alpha\sin\theta_k + \dfrac{\sqrt{2}}{2}\beta\right)}{\alpha\cos\theta_k} - t'\tan\theta_o, \\ y = \dfrac{\dfrac{\sqrt{2}}{2}\beta t'}{\alpha\cos\theta_k}. \end{cases} \tag{36}$$

3.2.2. Simulation relationship between incident angle and dispersion

Letting the half-wave plate be of quartz crystal, $n_1 = 1.53000$, $n_o' = 1.54424$, $n_e' = 1.55335$, $t' = 1.973$ mm, the dispersion curve is shown in Fig. 4. From the figure, the absolute values of dispersion in the x direction and the dispersion in the y direction become bigger with incident angle increasing from 0 to 2 rad. Increasing incident angle is one of methods to improve the SLPIIS.

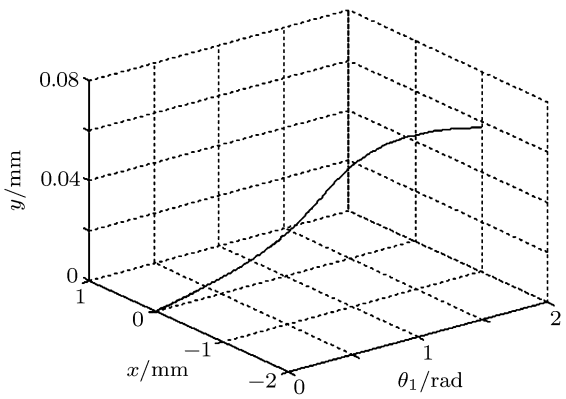


Fig. 4. Relation curve between incident angle and dispersion in the half-wave plate.

3.3. Relationship between incident angle and dispersion in the right plate of modified Savart polariscope

The optical axis direction of the right plate in modified Savart polariscope is

$$\boldsymbol{e}_p = \frac{\sqrt{2}}{2}\boldsymbol{i} - \frac{\sqrt{2}}{2}\boldsymbol{k}. \tag{37}$$

The values of θ_p and φ_p are

$$\begin{cases} \theta_p = \dfrac{3\pi}{4}, \\ \phi_p = 0. \end{cases} \tag{38}$$

The angle of refraction is

$$\theta_o = \arcsin(n_1 \sin\theta_1 / n_o), \tag{39}$$

where n_1 is the refractive index of the adherent.

3.3.1. Calculation relationship between incident angle and dispersion

The direction of e-wave vector is

$$\boldsymbol{e}_k = \sin\theta_k \boldsymbol{i} + \cos\theta_k \boldsymbol{k}. \tag{40}$$

Let

$$A_1 = n_1 \sin\theta_1, \tag{41}$$

$$A = n_o^2 n_e^2 - \frac{1}{2}A_1^2\left(n_e^2 + n_o^2\right), \tag{42}$$

$$B = A_1^2\left(n_o^2 - n_e^2\right), \tag{43}$$

$$C = \frac{1}{2}A_1^2\left(n_e^2 + n_o^2\right), \tag{44}$$

where θ_k satisfies the following relationship:

$$\tan\theta_k = \frac{1}{2A}\left(B + \sqrt{B^2 + 4AC}\right). \tag{45}$$

The direction of e-ray is

$$\boldsymbol{e}_r = \left(\alpha\sin\theta_k - \frac{\sqrt{2}}{2}\beta\right)\boldsymbol{i} + \left(\alpha\cos\theta_k - \frac{\sqrt{2}}{2}\beta\right)\boldsymbol{k}. \tag{46}$$

Let the thickness of the right plate be t, then the coordinate of output o-ray will be

$$\begin{cases} x_o = t\tan\theta_o, \\ y_o = 0, \\ z_o = t. \end{cases} \tag{47}$$

The coordinate of output e-ray is

$$\begin{cases} x_e = r\left(\alpha\sin\theta_k - \dfrac{\sqrt{2}}{2}\beta\right), \\ y_e = 0, \\ z_e = r\left(\alpha\cos\theta_k - \dfrac{\sqrt{2}}{2}\beta\right). \end{cases} \tag{48}$$

The dispersion is

$$x = \frac{t\left(\alpha\sin\theta_k - \dfrac{\sqrt{2}}{2}\beta\right)}{\alpha\cos\theta_k - \dfrac{\sqrt{2}}{2}\beta} - t\tan\theta_o. \tag{49}$$

3.3.2. Simulation relationship between incident angle and dispersion

For $n_1 = 1.53000$, $n_o = 1.65835$, $n_e = 1.48640$, and $t = 6$ mm, the dispersion curve is shown in Fig. 5. From the figure, the dispersion becomes bigger with the incident angle increasing from 0 to 1.6 rad.

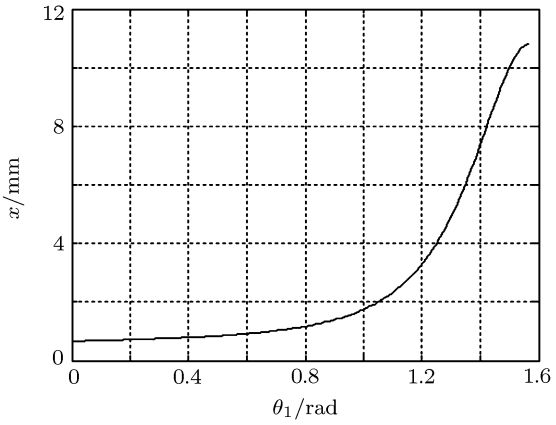


Fig. 5. Relation between incident angle and dispersion in the right plate.

4. Conclusions

Based on the extension of Snell's law, the dispersions of e-ray and o-ray in the modified Savart polariscope are obtained by calculation and simulation. In the left plate of the modified Savart polariscope, the dispersion occurs only in the x direction. The dispersion increases with the incident angle increasing. The dispersion occurs in the x and the y directions in the right plate of the Savart polariscope. In the x direction, the dispersion increases in a positive direction with the incident angle increasing. In the y direction, the dispersion augments in a negative direction with the incident angle increasing. These results may provide a way to improve image quality by increasing the incident angle, thereby improving the performance of SLPIIS.

References

[1] Zhang C M, Xiang L B and Zhao B C In: 2000 Lessard R A and Lampropoulos G A (eds). *Applications of Photonic Technology* 4 *Proc. SPIE* **4087** 957

[2] Zhang C M, Xiang L B and Zhao B C 2004 *J. Opt.* A: *Pure Appl. Opt.* **6** 1

[3] Zhang C M, Xiang L B and Zhao B C 2002 *Opt. Commun.* **203** 21

[4] Zhang C M, Zhao B C and Xiang L B 2003 *Opt. Commun.* **227** 221

[5] Zhang C M *Static Polarization Interference Imaging Spectrometer* Chinese Patent 01213109.1, 27 February 2002

[6] Zhang C M, Zhao B C and Xiang L B 2004 *Appl. Opt.* **43** 6090

[7] Francon M and Mallick S 1971 *Polarized Interferometer* (New York: Wiley) pp24–25, pp139–140

[8] Wu J F, Zhang C M, Zhang Y T, Liu H C and Zhai X J 2008 *Chin. Phys.* B **17** 2504

[9] Wu J F, Zhang C M, Yue R H and Li R L 2005 *Commun. Theor.* **43** 687

[10] Wu J F and Liu H C 2009 *Acta Opt. Sin.* **29** 93 (in Chinese)

[11] Wu J F and Zhang C M 2009 *Sci. China Ser.* G **52** 1003

[12] Wu J F, Sun M Z and Zhang C M 2009 *Acta Phys. Sin.* **58** 3844 (in Chinese)

[13] Wu J F and Zhang C M *Optik* http://dx.doi.org/10.1016/j.ijleo.2009.05.005.

[14] Zhang C M, Zhao B C, Yuan Z L and Huang W J 2009 *J. Opt.* A: *Pure Appl Opt.* **11** 085401

[15] Wu J F and Liu H C 2009 *Proc. SPIE* **7279** 72790R-1